JOURNAL OF AGRICULTURAL AND FOOD CHEMISTRY

ARTICLE

pubs.acs.org/JAFC

Metabolite Profiling of *Angelica gigas* from Different Geographical Origins Using ^{1}H NMR and UPLC-MS Analyses

Eun Jin Kim,[†,‡,∥] Joseph Kwon,[§,∥] Seong Hwa Park,[§] Chiyoul Park,[■] Young-Bae Seo,[⊗] Hyun-Kyoo Shin,[▼] Ho Kyoung Kim,[▼] Kwang-Sik Lee,[⊥] Sang-Yun Choi,[‡] Do Hyun Ryu,[●] and Geum-Sook Hwang[*,†,△]

[†]Seoul Center, Korea Basic Science Institute, Seoul 136-713, Republic of Korea

[‡]School of Life Science and Biotechnology, Korea University, Seoul 136-701, Republic of Korea

[§]Gwangju Center, Korea Basic Science Institute, Gwangju 500-757, Republic of Korea

[■]Waters Company Korea, Seoul 188-5, Republic of Korea

[⊗]Department of Herbalogy, College of Oriental Medicine, Daejeon University, Daejeon 300-716, Republic of Korea

[▼]Herbal Medicine EBM Research Center, Korea Institute of Oriental Medicine, Daejeon 305-811, Republic of Korea

[⊥]Division of Earth and Environmental Science, Korea Basic Science Institute, Deajeon 305-333, Republic of Korea

[●]Department of Chemistry, Sungkyunkwan University, Suwon 440-746, Republic of Korea

[△]Graduate School of Analytical Science and Technology, Chungnam National University, Daejeon 305-764, Republic of Korea

ABSTRACT: *Angelica gigas* obtained from different geographical regions was characterized using ^{1}H nuclear magnetic resonance (NMR) spectroscopy and ultraperformance liquid chromatography−mass spectrometry (UPLC-MS) followed by multivariate data analyses. Principal component analysis (PCA) and orthogonal partial least-squares-discriminant analysis (OPLS-DA) score plots from ^{1}H NMR and UPLC-MS data sets showed a clear distinction among *A. gigas* from three different regions in Korea. The major metabolites that contributed to the discrimination factor were primary metabolites including acetate, choline, citrate, 1,3-dimethylurate, fumarate, glucose, histamine, lactose, malate, *N*-acetylglutamate, succinate, and valine and secondary metabolites including decursin, decursinol, nodakenin, marmesin, 7-hydroxy-6-(2*R*-hydroxy-3-methylbut-3-ethyl)coumarin in *A. gigas* roots. The results demonstrate that ^{1}H NMR and UPLC-MS-based metabolic profiling coupled with chemometric analysis can be used to discriminate the geographical origins of various herbal medicines and to identify primary and secondary metabolites responsible for discrimination.

KEYWORDS: metabolite profiling, *Angelica gigas*, geographical origin, ^{1}H NMR, UPLS-MS, chemometric analysis

INTRODUCTION

Dang Gui (*Angelica gigas*), an oriental herbal medicine, has been widely used in the treatment of anemia, hypertension, chronic bronchitis, asthma, rheumatism, and cardiovascular diseases.[1−3] Knowledge of the regional origin of the herb and product quality control is important. Dang Gui has been studied extensively and is known to contain many components that effectively treat diseases.[4] In particular, coumarins, such as decursin, decursinol, and nodakenin, are the major constituents of *A. gigas*.[5−7] The quality of herbal medicines such as Dang Gui is influenced by environmental factors, such as temperature, sun exposure time, rainfall, and soil. Determination of quality criteria for herbal medicine based on well-controlled methodologies is important for ensuring safety and efficacy.

Metabolite profiling and fingerprinting analyses using spectroscopic and spectrometric techniques, such as ^{1}H nuclear magnetic resonance (NMR) spectroscopy and liquid chromatography−mass spectrometry (LC-MS), have been used in combination to determine the identity and relative amounts of components from specific herbal extracts.

Currently, a variety of metabolic profiling techniques is used routinely, and new methods are also being developed for metabonomic[8−10] and metabolomic studies.[11,12] Metabolite fingerprinting by NMR is widely used for various plant-derived products, including ginseng,[13,14] green tea,[15,16] grapes or wine,[17−19] olive oil,[20] fruit juice,[21] and others.[22−24] Additionally, the use of ultraperformance liquid chromatography (UPLC)[25,26] and mass spectrometry (MS)[27,28] for metabolite profiling has been reported.

^{1}H NMR is well suited for metabolite profiling because it allows simultaneous detection of a diverse group of secondary metabolites in addition to abundant primary metabolites. In an NMR spectrum, signal intensity is proportional to molar concentration, enabling direct comparison among the concentrations of all compounds without the need for calibration curves. Additionally, rapid, high-throughput, and high-sensitivity analysis has resulted in ultrafast separation and identification using LC-MS techniques.[29,30] Among the various LC platforms, UPLC is considered to be suitable for global metabolite profiling by providing reproducible retention time.[31] The ability to generate high peak capacities in a short time by

Received: April 24, 2011
Revised: July 19, 2011
Accepted: July 21, 2011
Published: July 21, 2011

dx.doi.org/10.1021/jf2016286 | *J. Agric. Food Chem.* 2011, 59, 8806–8815

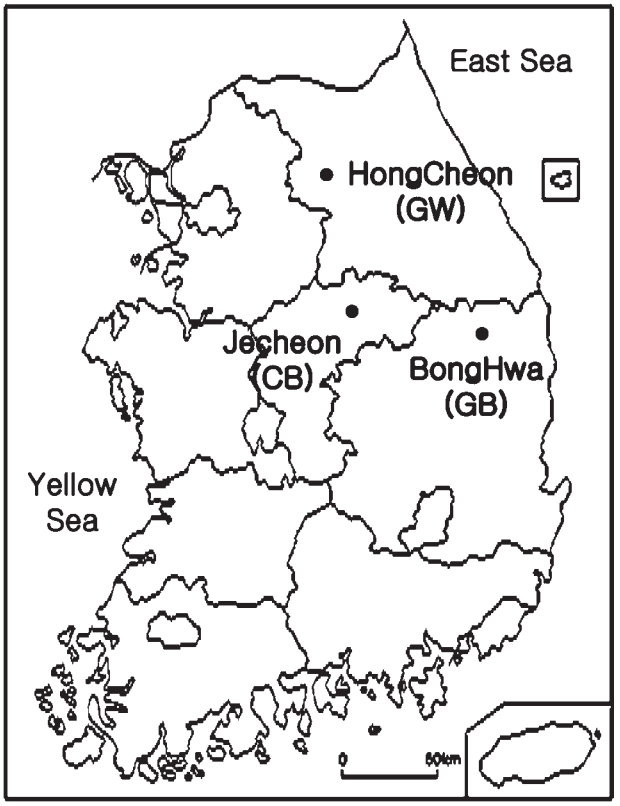

Figure 1. Geographical regions of *Angelica gigas* growth in Korea. Abbreviations: GW, Hongcheon-gun of Gangwon-do, Korea; GB, Bonghwa-gun of Gyeongsangbuk-do, Korea; CB, Jecheon-si of Chungcheongbuk-do, Korea.

UPLC has facilitated the simultaneous analysis of the complex samples with diverse chemical characteristics.[32,33]

In this study, ^{1}H NMR and UPLC-MS were used to determine the metabolic profiles of *A. gigas* from three different regions. The semipolar metabolite contents of *A. gigas* were extracted using methanol as an extraction solvent. The extracts of *A. gigas* were analyzed by ^{1}H NMR and UPLC-MS to discriminate their geographical origins and to detect marker metabolites of *A. gigas*, depending on origin, climate, cultivation, and the growth stage at cultivation. Our study provides insight into the metabolite profiling using a combination of NMR and UPLC-MS as a reliable and complete approach for presenting complementary information on primary and secondary metabolites in herbal medicines.

MATERIALS AND METHODS

Plant Material and Chemicals. *A. gigas* roots were obtained from Hongcheon-gun of Gangwon-do (GW), Bonghwa-gun of Gyeongsangbuk-do (GB), and Jecheon-si of Chungcheongbuk-do (CB) in South Korea (Figure 1).[34] Twenty biologically different *A. gigas* roots were collected from each region, and 60 samples for three regions were used in this study. Twenty samples within the same region were prepared from 20 different plants collected in different locations of the same garden. All samples were stored at −80 °C until required for analysis. All samples for the three different regions were harvested in October and genetically identical.

Methanol-d_4 (99.8%), purchased from Sigma-Aldrich, and deuterium oxide (D_2O, 99.9%), from Cambridge Isotope Laboratories, Inc., were used as NMR solvents. Acetonitrile and water (HPLC grade) were purchased from Burdick & Jackson, and formic acid was from Sigma-Aldrich.

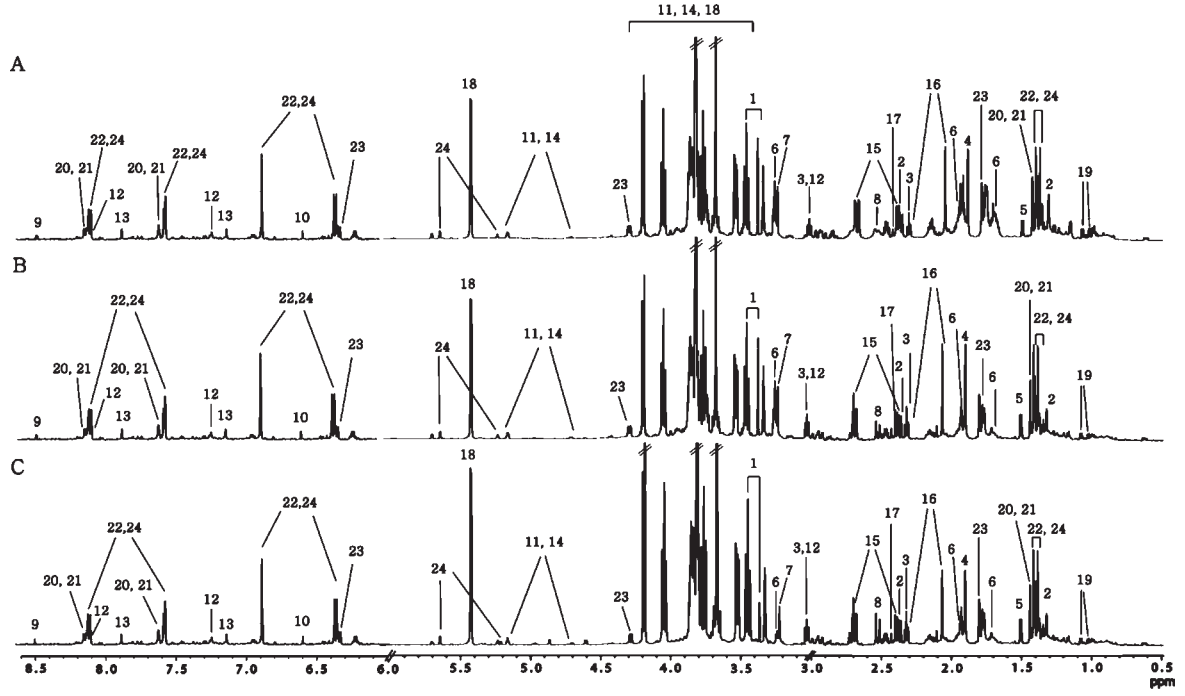

Figure 2. Representative ^{1}H NMR spectra of *Angelica gigas* harvested from three different regions in Korea: Hongcheon-gun of Gangwon-do (A), Bonghwa-gun of Gyeongsangbuk-do (B), and Jecheon-si of Chungcheongbuk-do (C). Peaks: 1, 1,3-dimethylurate; 2, 2-hydroxy-3-methylglutarate; 3, 4-aminobutyrate; 4, acetate; 5, alanine; 6, arginine; 7, choline; 8, citrate; 9, formate; 10, fumarate; 11, glucose; 12, histamine; 13, histidine; 14, lactose; 15, malate; 16, *N*-acetylglutamate; 17, succinate; 18, sucrose; 19, valine; 20, nodakenin; 21, marmesin; 22, decursinol; 23, 7-hydroxy-6-(2*R*)-hydroxy-3-methylbut-3-ethyl)coumarin; 24, decursin.

dx.doi.org/10.1021/jf2016286 |*J. Agric. Food Chem.* 2011, 59, 8806–8815

Table 1. Chemical Shift and Quantification of Metabolites Identified in the ^{1}H NMR Spectra of *Angelica gigas* from Three Regions

metabolite[b]	chemical shift (ppm)	mean (n^a = 20) ± standard error (μM)		
		GW	GB	CB
1,3-dimethylurate[a,b]	3.3 (s), 3.4 (s)	886.0 ± 107.2	1956 ± 163.0	1142 ± 86.95
3-hydroxy-3-methylglutarate	1.3 (s), 2.4 (q)	314.4 ± 26.00	326.0 ± 19.40	315.7 ± 32.58
4-aminobutyrate	1.9 (m), 2.3 (t), 3.0 (t)	1128 ± 117.7	868.1 ± 52.27	961.5 ± 86.09
acetate[a,b]	1.9 (s)	831.9 ± 56.99	400.7 ± 28.40	903.1 ± 118.3
alanine	1.5 (d), 3.8 (q)	1051 ± 74.28	995.2 ± 47.83	1164 ± 43.20
arginine	1.7 (m), 1.9 (m), 3.2 (t), 3.7 (t)	7465 ± 771.9	5489 ± 626.2	6063 ± 880.9
choline[a,b]	3.2 (s), 3.5 (b), 4.0 (b)	953.5 ± 56.20	791.5 ± 22.61	1029 ± 21.45
citrate[a,b,c]	2.5 (d), 2.7 (d)	792.2 ± 150.0	2207 ± 244.9	3184 ± 230.4
formate	8.5 (s)	403.0 ± 33.13	309.0 ± 16.62	327.7 ± 17.32
fumarate[a,b]	6.5 (s)	421.8 ± 56.02	194.4 ± 29.63	530.5 ± 74.82
glucose[a]	3.2 (t), 3.4 (m), 3.5 (q), 3.7 (b), 4.7 (d), 5.2 (d)	1943 ± 175.9	2365 ± 152.4	2861 ± 162.0
histamine[a,c]	3.0 (t), 3.4 (t), 7.1 (s), 7.8 (s)	693.8 ± 50.89	1047 ± 81.43	912.0 ± 55.59
histidine	3.2 (m), 4.0 (q), 7.1 (s), 7.8 (s)	1617 ± 232.5	1679 ± 177.6	1758 ± 186.6
lactose[a,b]	3.2 (t), 3.5−4.0 (b), 4.6 (d), 4.7 (d), 5.2 (d)	2452 ± 242.4	3880 ± 138.0	2945 ± 272.8
malate[b,c]	2.4 (q), 2.7 (d,d), 4.3 (d)	5145 ± 615.6	6333 ± 446.4	13551 ± 1038
N-acetylglutamate[c]	1.9 (m), 2.0 (s), 2.3 (t), 4.1 (m), 7.9 (b)	723.4 ± 67.75	967.9 ± 77.97	1160 ± 84.13
succinate[b,c]	2.4 (s)	172.8 ± 14.91	170.2 ± 6.133	220.0 ± 14.42
sucrose	3.4 (t), 3.5 (d,d), 3.6 (s), 3.7 (t), 3.8 (m), 4.0 (t), 4.2 (d), 5.4 (d)	47824 ± 3334	53148 ± 2337	64035 ± 1662
valine[a,b]	1.0 (d), 1.1 (d), 2.2 (m), 3.6 (d)	344.1 ± 23.38	250.2 ± 17.55	349.2 ± 11.46

[a] The number of samples (n) used for quantification. [b] Letters a, b, and c above the metabolites name indicate pairwise difference identified by Tukey−Kramer multiple-comparison tests (a, GW vs GB; b, GB vs CB; c, CB vs GW).

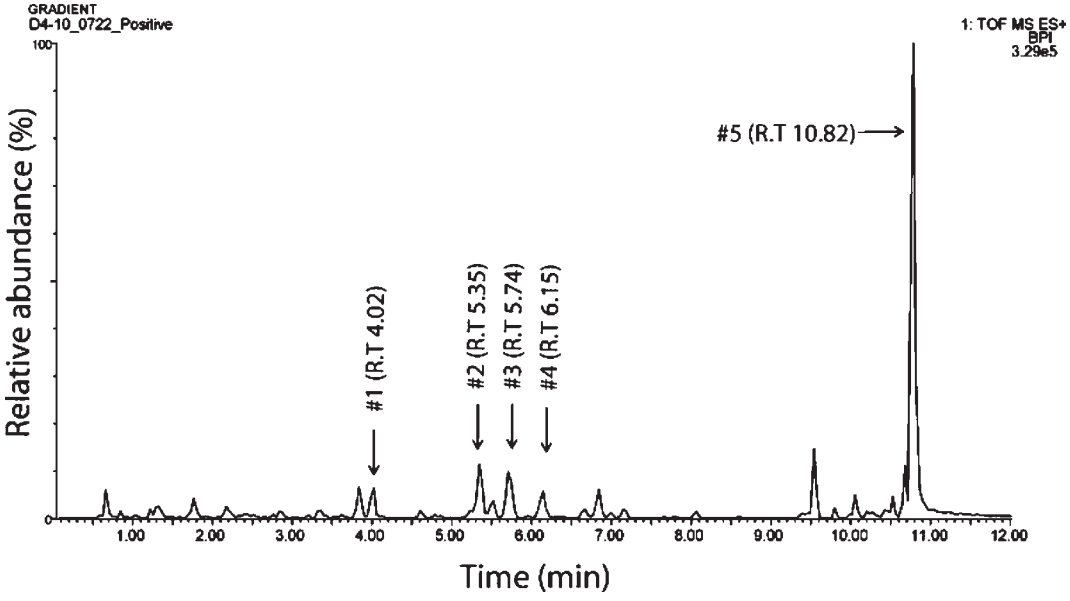

Figure 3. ES+ base peak intensity (BPI) chromatogram from a UPLC-MS chromatogram of *Angelica gigas*. #1, nodakenin; #2, marmesin; #3, decursinol; #4, 7-hydroxy-6-(2*R*)-hydroxy-3-methylbut-3-ethyl)coumarin; #5, decursin.

Sample Preparation for NMR and UPLC-MS Analyses. *A. gigas* roots were freeze-dried and ground to a fine powder. Five hundred microliters of methanol-d_4 (99.8%), 400 μL of 0.2 M phosphate buffer solution (0.2 M Na_2HPO_4, 0.2 M NaH_2PO_4 in D_2O, pH 7.0), and 100 μL of 5 mM 2,2-dimethyl-2-silapentane-5-sulfonic acid (DSS, 97%) were added to 100 mg of dried powder as extraction solvents. D_2O was used for the internal lock signal and DSS as the internal standard with a chemical shift (δ) of 0.0 ppm. The extracts were sonicated for 20 min, followed by centrifugation (10 min, 16609g) at room temperature and adjusted to pH 7.0 ± 0.5 using 1 mM NaOH and 1 mM HCl. The extract (600 μL) was transferred to 5 mm NMR tubes for NMR analysis.

For UPLC-MS analysis, the same extracts used for ^{1}H NMR were evaporated in vacuo followed by the addition of 10 mL of methanol. Filtration through a 0.2 μm membrane filter prior to analysis was carried out to protect the UPLC column used under high pressure. Sample solutions were centrifuged (20 min, 4 °C, 3500 rpm) and filtered

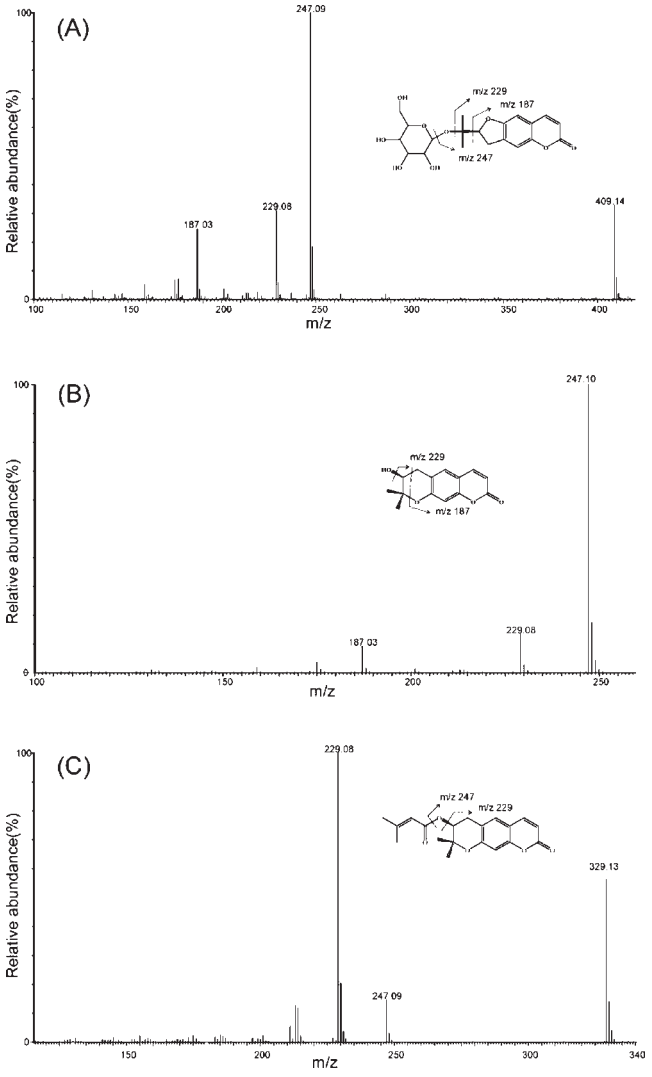

Figure 4. ESI MS/MS fragmentation pattern of nodakenin at m/z 409 (A), decursinol at m/z 247 (B), and decursin at m/z 329 (C).

through a 0.2 μm membrane filter prior to analysis. The injection volume of the sample was 5 μL.

NMR Spectroscopy. ^{1}H NMR spectra were acquired on a VNMRS 600 MHz NMR spectrometer (Varian Inc., Palo Alto, CA) using a triple-resonance 5 mm HCN salt-tolerant cold probe. ^{1}H NMR spectra were acquired using the NOESY PRESAT pulse sequence, which was applied to suppress the residual water signal. Thirty-two scans were collected into 67568 data points using a spectral width of 8445.9 Hz, a relaxation delay of 2.0 s, an acquisition time of 4.0 s, and a mixing time of 100 ms. A 0.5 Hz line-broadening function was applied to all spectra for Fourier transformation (FT) followed by phasing and baseline correction. Signal assignment for representative samples was achieved using two-dimensional (2D) total correlation spectroscopy (TOCSY), heteronuclear multiple-bond correlation (HMBC), heteronuclear single-quantum correlation (HSQC), Chenomx NMR suite 6.0, 600 MHz (pH 6.0−8.0) database, spiking experiments, and comparison with literature values.

UPLC Conditions. The LC-MS profiling experiments were performed on an Acquity UPLC system (Waters Co., Milford, MA) equipped with a binary solvent delivery system and an autosampler. Chromatographic separation was carried out on an Acquity UPLC BEH C18 column (100 × 2.1 mm, 1.7 μm, 40 °C). The mobile phase consisted of 0.1% formic acid in 10% acetonitrile as solvent A and 0.1% formic acid in 90% acetonitrile as solvent B. Separation was performed by gradient elution with 95% A for 0 min, 20% A for 10 min, 0% A for 13.5 min, and 95% A for 15 min at a flow rate of 400 μL/min. The injection volume of the sample was 5 μL.

MS Conditions. Accurate mass measurements and MS/MS fragmentation analysis were performed with a Synapt high-definition mass spectrometry system (HDMS; Waters Co.). Electrospray ionization (ESI) mass spectra were acquired in positive and negative ionization modes by scanning over the m/z range of 100−1800. The ESI capillary voltage was set at 3.1 kV. The temperatures of the electrospray source and desolvation gas were 100 and 300 °C, respectively. Leucine-enkephalin was used as an independent reference lock-mass via the LockSpray to ensure mass accuracy and reproducibility. The collision energy was varied from 15 to 45 V in an energy-lamping mode.

^{1}H NMR Data Analysis. All NMR spectra were phase-adjusted and baseline-corrected using the Chenomx NMR suite 6.0 software, professional edition (Chenomx Inc., Edmonton, Canada). Each NMR spectrum was bucketed by integrating regions having an equal bin size of 0.005 ppm over a δ range of 0.7−9.5. All shifts related to the solvent (i.e., in the ranges of 3.28−3.33 ppm and 4.74−4.90 ppm) and DSS were eliminated. The spectra were then normalized to the total spectral area and exported as a text file for chemometric data. The text files were imported into SIMCA-P+ version 12.0 (Umetrics, Umeå, Sweden) for multivariate data analysis and Pareto-scaled to minimize the influence of baseline deviations and noise. A multivariate data analysis, principal component analysis (PCA), was initially performed to examine the intrinsic variation in the data set and obtain an overview of variation among the groups. Orthogonal partial least-squares-discriminate analysis (OPLS-DA) of the NMR spectral data was performed to differentiate among the group of samples.[35,36] The metabolites associated with the group separations were indicated by the corresponding S-plot, in which each point represented a single NMR spectral region segment.[37] In addition, we performed a permutation test and an external validation to test the validity of the OPLS-DA models.[38−40] *A. gigas* metabolites were quantified using the Chenomx NMR suite 6.0 software, which compares the integral of a known reference signal (DSS) with the signal derived from a library of compounds containing chemical shifts and peak multiplicities for all of the resonances of compound.

UPLC-MS Data Analysis. Extracts of *A. gigas* were analyzed to identify potential variables that could be used to discriminate the regions of origin using a UPLC coupled with quadrupole time-of-flight (Q-TOF) MS. Peak finding, peak alignment, and peak filtering of raw data were carried out using MarkerLynx applications manager (ver. 4.1; Waters, Manchester, U.K.) with the following parameters: data collection parameters were set as intensity threshold 80 counts, mass window at 0.04 Da, retention time window of 0.15 min, and noise elimination level at 5. Normalized peak area matrices were exported to SIMCA-P+ (ver. 12.0; Umetrics) for multivariate statistical analysis. The intensity of each precursor ion was analyzed by PCA. The detailed data analysis for multivariate statistics is similar to that of NMR data analysis.

Statistical Methods. A one-way analysis of variance (ANOVA) was performed using GraphPad PRISM (ver. 5.0; GraphPad Software, Inc.) and SPSS 12.0 (LEAD Technologies, Inc.) to test the significance of differences in metabolite levels among *A. gigas* from different regions. Tukey multiple-comparison tests were performed to reveal pairwise differences. For all analyses, the critical p value was set at 0.05.

RESULTS AND DISCUSSION

^{1}H NMR Analysis. Representative one-dimensional ^{1}H NMR spectra of aqueous *A. gigas* samples from three different regions are shown in Figure 2. A visual comparison revealed similarities among all spectra, suggesting similar metabolic profiles among

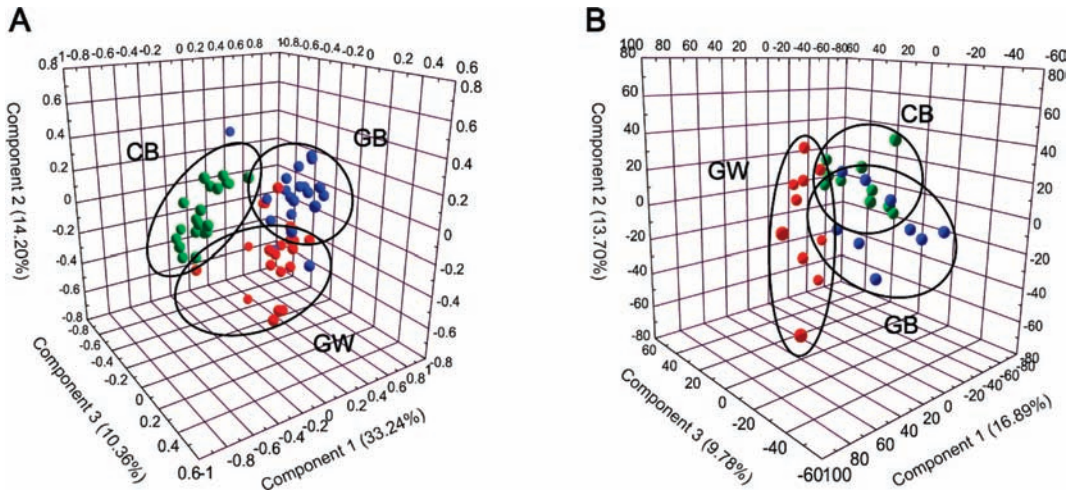

Figure 5. PCA score three-dimensional plot derived from ^{1}H NMR (A) and UPLC-MS (B). Abbreviations: GW, Hongcheon-gun of Gangwon-do, Korea; GB, Bonghwa-gun of Gyeongsangbuk-do, Korea; CB, Jecheon-si of Chungcheongbuk-do, Korea.

A. gigas from the different regions. The analysis of *A. gigas* extracts by ^{1}H NMR allowed the detection of essential primary metabolites and several secondary metabolites. Primary metabolites, such as sugars, amino acids, organic acids, and nucleotides, indicate a high natural concentration of metabolites in the roots. Secondary metabolites, such as coumarin derivatives, were more difficult to detect than primary metabolites.

Sugar compounds were observed primarily between δ 3.00 and 5.50. Sucrose was detected as a major disaccharide. Lactose and glucose were also observed in *A. gigas*. Several organic compounds, including 3-hydroxy-3-methylglutarate, 4-aminobutyrate (GABA), acetate, choline, citrate, formate, fumarate, malate, *N*-acetylglutamate, succinate, and 1,3-dimethylurate, and amino acids, including alanine, arginine, histidine, histamine, and valine, were detected in *A. gigas* samples. Additionally, coumarin derivatives, including decursin, decursinol, nodakenin, marmesine, and 7-hydroxy-6-(2*R*)-hydroxy-3-methylbut-3-enyl)-coumarin, were observed in the NMR spectra and identified by comparing spiking experiments and 2D NMR. The chemical shifts of the identified metabolites by NMR are listed in Table 1.

UPLC-MS Analysis. UPLC-MS is a rapid, effective, and convenient analytical method for the detection of compounds present in *A. gigas* from different regions. Figure 3 shows one of the typical total ion chromatograms (TIC)s of the *A. gigas* root samples from each region. Each chromatogram of the *A. gigas* root samples from three regions detected the five secondary metabolites. These metabolites showed similar patterns of separation in chromatography and were identified according to the mass spectrum and retention time. By comparison of the mass spectra with NMR, several peaks were identified, including nodakenin, marmesin, decursinol, 7-hydroxy-6-(2*R*)-hydroxy-3-methylbut-3-enyl)coumarin, and decursin. [41,42]

In this study, the exact masses and retention times of individual components from *A. gigas* extracts were measured in both positive and negative ionization modes using an autosampler-equipped UPLC-MS system. The positive ionization mode provided the best sensitivity and much higher ionization efficiency for the five coumarin derivatives compared with the negative ionization mode. The ESI MS/MS fragmentation spectra of the three coumarin derivatives are shown in Figure 4. For nodakenin (Figure 4A), the fragment ion at m/z 247 $[M + H - C_6H_{11}O_5]^+$ was prominent in the MS^2 spectrum of the ion at m/z 409 $[M + H]^+$. Decursinol (Figure 4B) exhibited a precursor ion peak at m/z 247 with fragment ion peaks at m/z 229 $[M + H - H_2O]$ and 187 $[M + H - C_3H_7O]^+$. Decursin (Figure 4C) displayed a precursor peak at m/z 329 $[M + H]^+$ and fragment ion peaks at m/z 247 and 229 due to the loss of an isoprenyl moiety (82 Da) and a water molecule (18 Da).[43]

Chemometric Data Analysis. PCA score plots were used to determine whether the metabolic fingerprint of each *A. gigas* sample was sufficiently unique to distinguish the different geographical regions and identify the biomarkers for each location. Each point in the score plots represents an individual sample, and samples exhibiting similar variances were clustered together. The PCA score plots derived from the NMR and UPLC-MS spectra are shown in Figure 5, panels A and B, respectively. The PCA 3D score plots revealed moderate separation between *A. gigas* samples (R^2 = 0.805, Q^2 = 0.62 for NMR and R^2 = 0.516, Q^2 = 0.103 for UPLC-MS). The low Q^2 value in UPLC-MS indicates the model is probably overfitted.

In NMR data, OPLS-DA score plots of two regions showed the obvious clustering of *A. gigas* samples in terms of their cultivation region in the OPLS 1. The samples grown in GW and GB (R^2 = 0.74, Q^2 = 0.92; Figure 6A), GW and CB (R^2 = 0.64, Q^2 = 0.91; Figure 6C), and GB and CB (R^2 = 0.58, Q^2 = 0.96; Figure 6E) were clearly separated. Statistically significant metabolites related to the differences between regions were selected from the S-plot. The axes plotted in the S-plot form the predictive component are the covariance $p[1]$ against the correlation $p(\mathrm{corr})[1]$. Therefore, variables in the dotted rectangles of Figure 6B,D,F contribute to the group separation and were considered as statistically significant metabolites. The S-plot of GW and GB (Figure 6B) shows that GW samples were higher in acetate, choline, fumarate, and valine. In contrast, GB samples were higher in citrate, 1,3-dimethylurate, histamine, and lactose. Figure 6D shows the comparisons between GB samples and CB samples. 1,3-Dimethylurate, histamine, and lactose were higher in GB samples, whereas acetate, choline, citrate, fumarate, malate, and succinate were higher in CB samples. In Figure 6F, acetate, choline, and valine were higher in GB samples, whereas citrate, glucose, malate, *N*-acetylglutamate, and succinate were higher in GB samples.

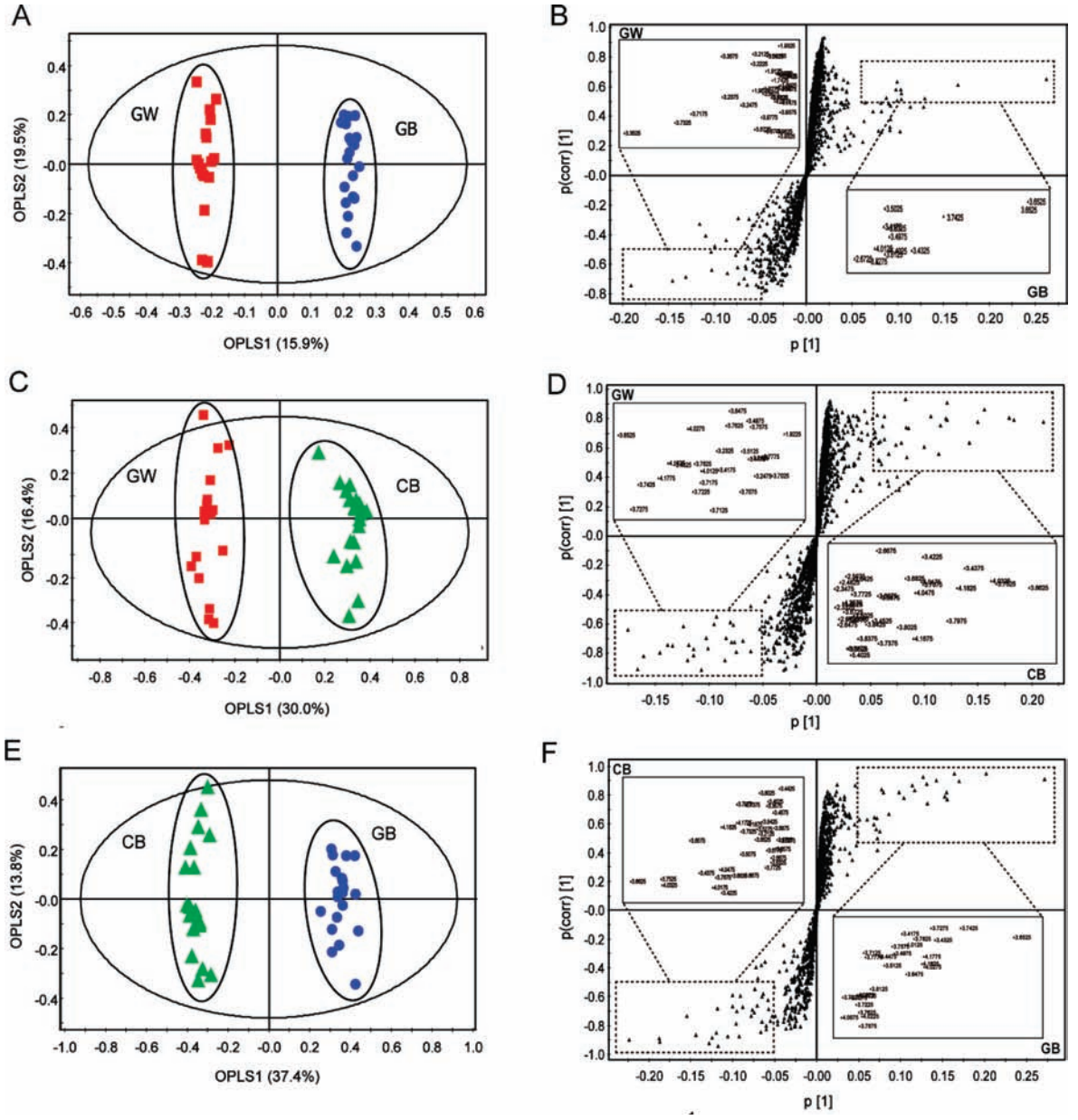

Figure 6. OPLS-DA score plots (A, C, and E) based on ^{1}H NMR spectra of root samples from *Angelica gigas* and S-plots (B, D, and F) of OPLS-DA from *A. gigas*. Cutoff values for the covariance of $p \geq |0.05|$ and for the correlation of $p(\mathrm{corr}) \geq |0.5|$ were used. The axes plotted in the S-plot form the predictive component are $p[1]$ versus $p(\mathrm{corr})[1]$; the names of metabolites corresponding to the variable are given in the text.

Furthermore, permutation tests were performed in the PLS-DA model to validate each OPLS-DA model. All Q^2 and R^2 values were higher in the permutation test than in the real model, revealing great predictability and goodness of fit. Additionally, the external validation was performed to validate OPLS-DA models. External validation aims to address the accuracy of a model in samples from different samples. For the prediction, the six samples (a test data set) were left randomly from each region (a training data set) and the OPLS-DA prediction model was peformed three times without them. The cutoff of the prediction was 0.5. As a result, almost all samples were correctly classified. In Figure 7B, the range of Ry^2 was 0.946−0.998 and that of Q^2 was 0.813−0.907. Between GW and CB (Figure 7D) Ry^2 was 0.987−0.998 and Q^2 was 0.926−0.958. In comparisons of GB and CB (Figure 7F), the range of Ry^2 was 0.969−0.991 and that of Q^2 was 0.922−0.959.

Quantitative Analysis of Metabolites. Figure 8 shows the scatter plots of identified metabolite levels in *A. gigas* from the three different regions. Acetate, choline, citrate, 1,3-dimethylurate, fumarate, histamine, lactose, and valine levels differed significantly between GW and GB samples. Also, GB and CB samples showed differences in acetate, choline, citrate, 1,3-dimethylurate, fumarate, lactose, malate, succinate, and valine levels. GW and CB samples exhibited differing levels of citrate, glucose, histamine, malate, *N*-acetylglutamate, and succinate. Quantification of five secondary metabolites is shown in Table 2. The level of marmesin was higher in GW compared to GB and CB, whereas the level of 7-hydroxy-6-(2-*R*)-hydroxy-3-methyl-but-3-ethyl)coumarin was higher in GB compared to GW and

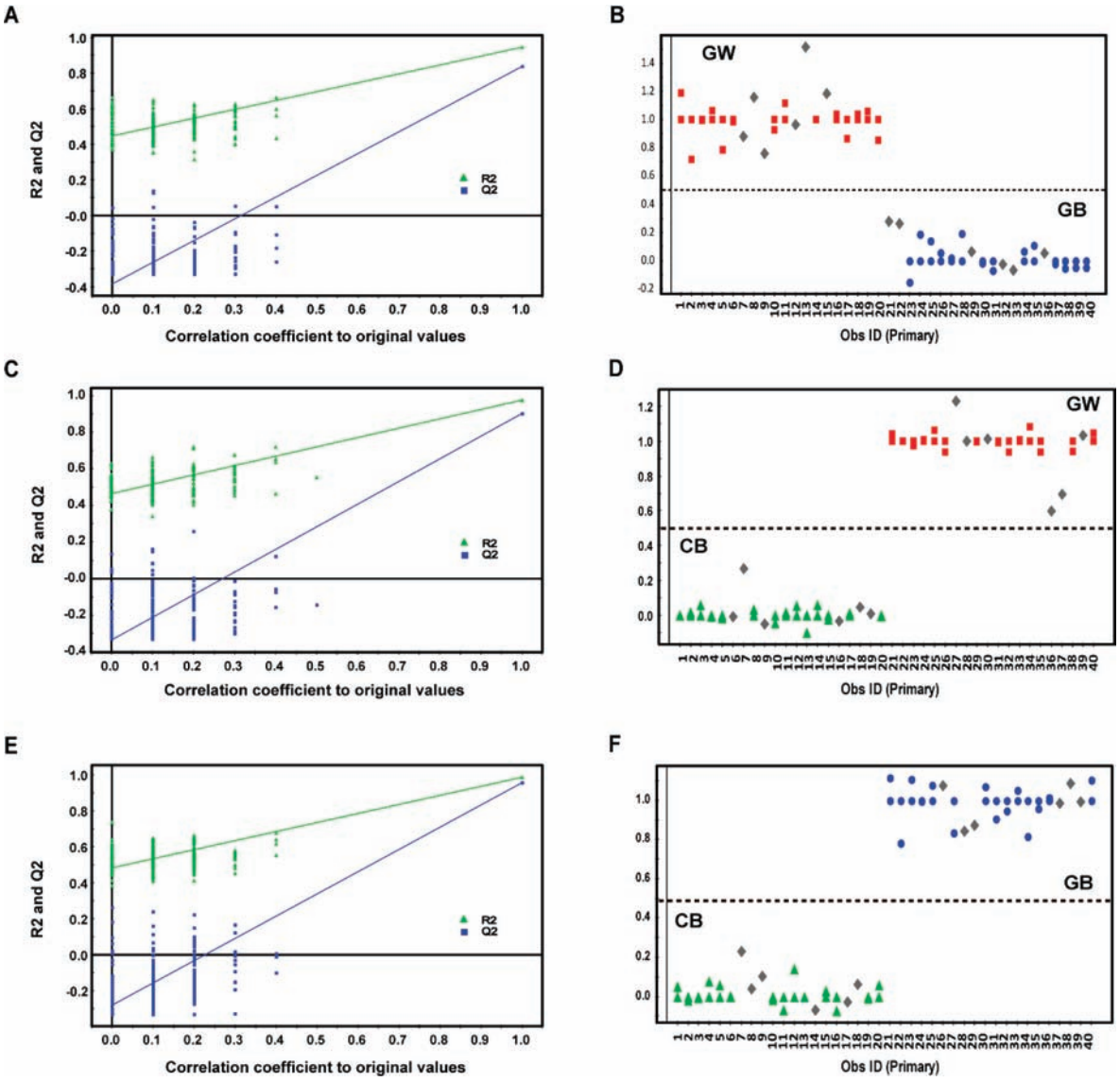

Figure 7. Results from the permutation tests, which were carried out with 200 random permutations in PLS-DA models from ^{1}H NMR spectra (A, C, and E) and external validation test of OPLS-DA models (B, D, and F): (A, B) GW versus GB; (C, D) GB versus CB; (E, F) GW versus CB.

CB. In contrast, levels of decursin and decursinol were higher in CB compared to other regions.

These metabolites contributed to the variance for discrimination of herbs according to the cultivation region. The variance was affected by various environmental factors in the cultivation region.

Metabolites in herbs are affected not only by climatic conditions but also by geographical conditions. The average daily temperatures were 17.6, 16.2, and 16.67 °C, average sun exposure times were 169.5, 173.4, and 170.0 h, and average rainfalls were 1527, 1353, and 1151 mm for GW, GB, and CB, respectively, from March to September of 2008. These data were obtained from the Korea Meteorological Administration. GW is located in the center of an inland peninsula in a mountain basin and has a combined mountain and continental climate. GB is located to the south of GW, west of the Taebaek Mountains, and a branch of the Taebaek Mountains. The Sobaek Mountains are west of GB. CB, which is located in the inland highlands, experiences frost and freeze earlier than the other two regions. These environmental factors can affect the metabolite levels in *A. gigas*. For example, citrate and malate levels differed according to the cultivated region; they were highest in CB because the region received the least rainfall, whereas they were lower in GW, which had the highest rainfall, the highest temperature, and the lowest sun exposure time. It has been reported that phosphoenolpyruvate carboxykinase (PEPCK) may play a role in the catabolism of malate and citrate.[44−46] PEPCK is an enzyme that decarboxylates part of the oxaloacetate formed in the Krebs cycle. Oxaloacetate can be transformed into glucose by gluconeogenesis, eliminating malate and citrate. It has reported that PEPCK activities are temperature dependent.[47] This study suggests that malate and citrate levels were strongly connected with each other; thus, they could also be key metabolites for regional discrimination.[17]

Additionally, it has been reported that the levels of reducing sugars and organic compounds in plants are dependent on temperature. At low temperatures, root respiration rates decrease and were negatively correlated to the concentrations

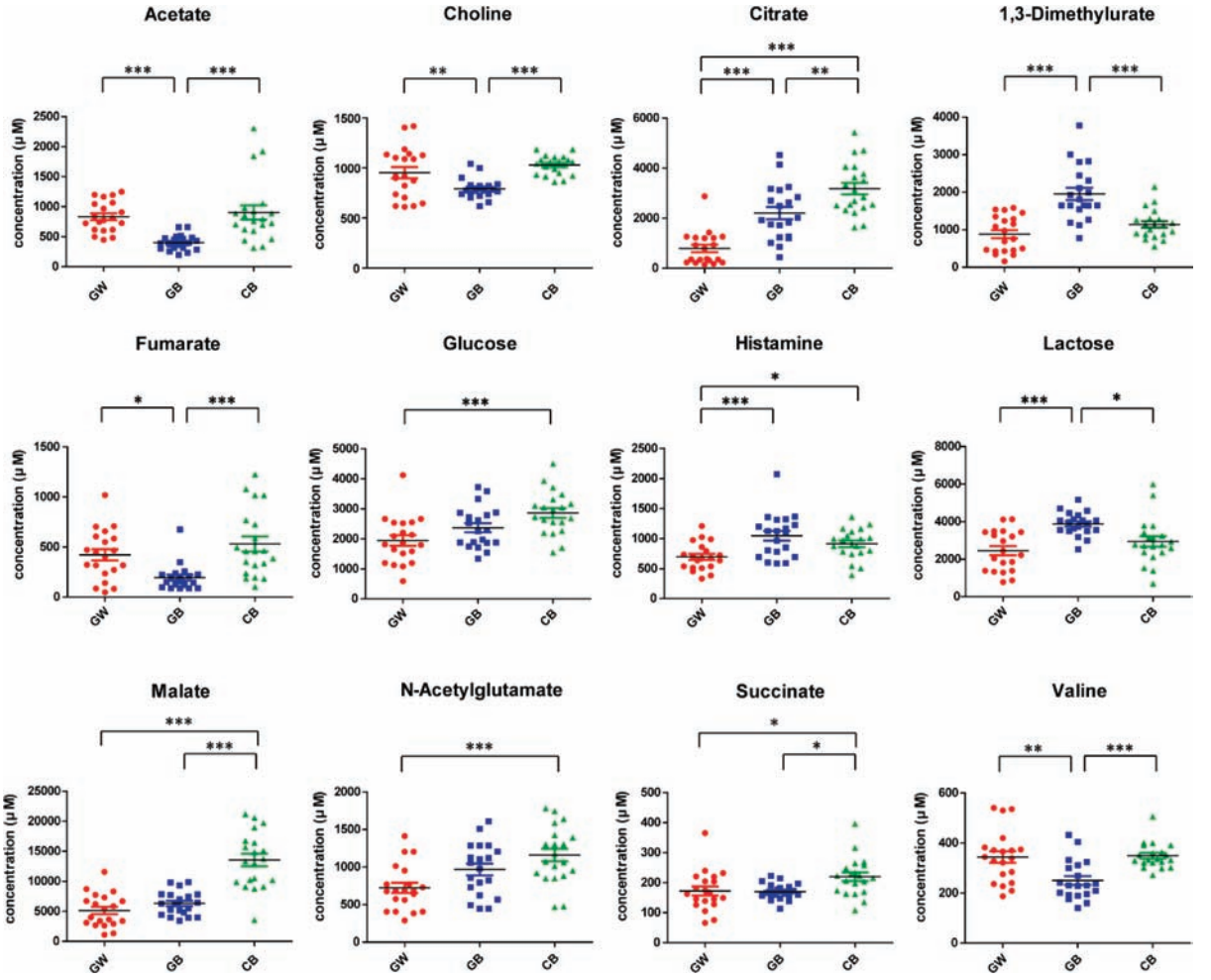

Figure 8. Quantification of metabolites identified from the root extract of *Angelica gigas* using ^{1}H NMR; scatter plots of significant metabolite concentration difference of *A. gigas* ($p < 0.05$). Data are given as the mean ± standard deviation.

Table 2. Retention Time (RT), Calculated Mass, and Peak Intensity of Metabolites Identified in UPLC-MS

			mean (n^a = 10) ± standard error (abundance)		
peak	RT (min)	obsd mass $[M + H]^+$	GW	GB	CB
nodakenin	4.02	409.1449	196.7 ± 13.20	191.1 ± 11.20	193.0 ± 7.080
marmesin	5.30	247.0970	268.5 ± 9.374	214.6 ± 23.92	196.4 ± 20.13
decursinol	5.70	247.0970	286.4 ± 33.22	310.8 ± 9.622	323.5 ± 6.831
7-hydroxy-6-(2*R*)-hydroxy-3-methylbut-3-ethyl)coumarin	6.15	247.0970	264.6 ± 24.12	295.9 ± 10.61	263.0 ± 6.603
decursin	10.80	329.1389	2484 ± 93.95	2412 ± 72.22	2608 ± 51.90

[a] The number of samples (n) used for quantification.

of reducing sugars and organic and inorganic compounds.[48,49] Thus, reducing sugars will accumulate while starch is consumed.[50] However, this was not confirmed by our data. Acetate, choline, fumarate, and valine levels were higher in GB compared with the other regions, whereas 1,3-dimethylurate, histamine, and lactose levels were lower in GB, which had the lowest temperature and the highest sun exposure time. Glucose, *N*-acetylglutamate, and succinate were found in high levels in CB.

In this study, we demonstrated that metabolite profiling using a combination of NMR and UPLC-MS coupled with multivariate analysis provides reliable and complete discrimination among *A. gigas* from three different regions in Korea by presenting complementary information on primary and secondary metabolites. Further investigation of metabolite profiling using chromatographic and spectroscopic tools could establish biomarkers for the discrimination of the geographical origins of herbal medicines. Reliable discrimination of the geographical origin of herbal medicine is important for consumers and producers. The combined application of ^{1}H NMR and LC-MS techniques is strongly recommended for quality control and, therefore, authentication of complex herbal medicines and products.

AUTHOR INFORMATION

Corresponding Author

*Postal address: Korea Basic Science Institute, Seoul 136-713, Korea. Phone: +82 2 920 0737. Fax: +82 2 920 0779. E-mail: gshwang@kbsi.re.kr.

Author Contributions

‖These authors contributed equally to the work.

Funding Sources

This work was supported by the National Research Foundation of Korea Grant funded by the Korean government (MEST) (2009, University-Institute cooperation program) and the Korea Basic Science Institute (T3173).

REFERENCES

(1) Lao, S. C.; Li, S. P.; Kan, K. K. W.; Li, P.; Wan, J. B.; Wang, Y. T.; Dong, T. T. X.; Tsim, K. W. K. Identification and quantification of 13 components in *Angelica sinensis* (Danggui) by gas chromatography−mass spectrometry coupled with pressurized liquid extraction. *Anal. Chim. Acta* **2004**, *526*, 131–137.

(2) Lin, L. Z.; He, X. G.; Lian, L. Z.; King, W.; Elliott, J. Liquid chromatographic−electrospray mass spectrometric study of the phthalides of *Angelica sinensis* and chemical changes of *Z*-ligustilide. *J. Chromatogr., A* **1998**, *810*, 71–79.

(3) Lu, G. H.; Chan, K.; Chan, C. L.; Leung, K.; Jiang, Z. H.; Zhao, Z. Z. Quantification of ligustilides in the roots of *Angelica sinensis* and related umbelliferous medicinal plants by high-performance liquid chromatography and liquid chromatography−mass spectrometry. *J. Chromatogr., A* **2004**, *1046*, 101–107.

(4) Jiang, C.; Lee, H. J.; Li, G.; Guo, J.; Malewicz, B.; Zhao, Y.; Lee, E. O.; Lee, J. H.; Kim, M. S. Potent antiandrogen and androgen receptor activities of an *Angelica gigas*-containing herbal formulation: identification of decursin as a novel and active compound with implications for prevention and treatment of prostate cancer. *Cancer Res.* **2006**, *66*, 453–463.

(5) Konoshima, M.; Chi, H. J.; Hata, K. Coumarins from the root of *Angelica gigas* Nakai. *Chem. Pharm. Bull.* **1968**, *16*, 1139–1140.

(6) Kang, Y. G.; Lee, J. H.; Chae, H. J.; Kim, D. H.; Lee, S.; Park, S. Y. HPLC analysis and extraction methods of decursin and decursinol angelate in *Angelica gigas* roots. *Kor. J. Pharmacogn.* **2003**, *34*, 201–205.

(7) Pachaly, P.; Treitner, A.; Sin, K. S. Neue Cumaringlykoside aus *Angelica gigas* [New coumarine glycosides from *Angelica gigas* roots]. *Pharmazie* **1996**, *51*, 57–61.

(8) Lindon, J. C.; Holmes, E.; Bollard, M. E.; Stanley, E. G.; Nicholson, J. K. Metabonomics technologies and their applications in physiological monitoring, drug safety assessment and disease diagnosis. *Biomarkers* **2004**, *9*, 1–31.

(9) Nicholson, J. K.; Connelly, J.; Lindon, J. C.; Holmes, E. Metabonomics: a platform for studying drug toxicity and gene function. *Nat. Rev. Drug Discov.* **2002**, *1*, 153–161.

(10) Nicholson, J. K.; Lindon, J. C.; Holmes, E. 'Metabonomics': understanding the metabolic responses of living systems to pathophysiological stimuli via multivariate statistical analysis of biological NMR spectroscopic data. *Xenobiotica* **1999**, *29*, 1181–1189.

(11) Kell, D. B. Metabolomics and systems biology: making sense of the soup. *Curr. Opin. Microbiol.* **2004**, *7*, 296–307.

(12) Weckwerth, W.; Fiehn, O. Can we discover novel pathways using metabolomic analysis? *Curr. Opin. Biotechnol.* **2002**, *13*, 156–160.

(13) Lee, E. J.; Shaykhutdinov, R.; Weljie, A. M.; Vogel, H. J.; Facchini, P. J.; Park, S. U.; Kim, Y. K.; Yang, T. J. Quality assessment of ginseng by ^{1}H NMR metabolite fingerprinting and profiling analysis. *J. Agric. Food Chem.* **2009**, *57*, 7513–7522.

(14) Kim, S. H.; Hyun, S. H.; Yang, S. O.; Choi, H. K.; Lee, B. Y. ^{1}H-NMR-based discrimination of thermal and vinegar treated ginseng roots. *J. Food Sci. 75*, C577-C581.

(15) Tarachiwin, L.; Koichi, U.; Kobayashi, A.; Fukusaki, E. ^{1}H NMR based metabolic profiling in the evaluation of Japanese green tea quality. *J. Agric. Food Chem.* **2007**, *55*, 9330–9336.

(16) Lee, J. E.; Lee, B. J.; Chung, J. O.; Hwang, J. A.; Lee, S. J.; Lee, C. H.; Hong, Y. S. Geographical and climatic dependencies of green tea (*Camellia sinensis*) metabolites: a ^{1}H NMR-based metabolomics study. *J. Agric. Food Chem.* **2010**, *58*, 10582−10589.

(17) Son, H. S.; Hwang, G. S.; Kim, K. M.; Ahn, H. J.; Park, W. M.; Van Den Berg, F.; Hong, Y. S.; Lee, C. H. Metabolomic studies on geographical grapes and their wines using ^{1}H NMR analysis coupled with multivariate statistics. *J. Agric. Food Chem.* **2009**, *57*, 1481–1490.

(18) Lee, J. E.; Hwang, G. S.; Van Den Berg, F.; Lee, C. H.; Hong, Y. S. Evidence of vintage effects on grape wines using ^{1}H NMR-based metabolomic study. *Anal. Chim. Acta* **2009**, *648*, 71–76.

(19) Son, H. S.; Hwang, G. S.; Ahn, H. J.; Park, W. M.; Lee, C. H.; Hong, Y. S. Characterization of wines from grape varieties through multivariate statistical analysis of ^{1}H NMR spectroscopic data. *Food Res. Int.* **2009**, *42*, 1483–1491.

(20) Rezzi, S.; Axelson, D. E.; Heberger, K.; Reniero, F.; Mariani, C.; Guillou, C. Classification of olive oils using high throughput flow ^{1}H NMR fingerprinting with principal component analysis, linear discriminant analysis and probabilistic neural networks. *Anal. Chim. Acta* **2005**, *552*, 13–24.

(21) Belton, P. S.; Delgadillo, I.; Holmes, E.; Nicholls, A.; Nicholson, J. K.; Spraul, M. Use of high-field ^{1}H NMR spectroscopy for the analysis of liquid foods. *J. Agric. Food Chem.* **1996**, *44*, 1483–1487.

(22) Tarachiwin, L.; Katoh, A.; Ute, K.; Fukusaki, E. Quality evaluation of *Angelica acutiloba* Kitagawa roots by ^{1}H NMR-based metabolic fingerprinting. *J. Pharm. Biomed. Anal.* **2008**, *48*, 42–48.

(23) Consonni, R.; Cagliani, L. R.; Stocchero, M.; Porretta, S. Triple concentrated tomato paste: discrimination between Italian and Chinese products. *J. Agric. Food Chem.* **2009**, *57*, 4506–4513.

(24) Choi, H.-K.; Choi, Y. H.; Verberne, M.; Lefeber, A. W. M.; Erkelens, C.; Verpoorte, R. Metabolic fingerprinting of wild type and transgenic tobacco plants by ^{1}H NMR and multivariate analysis technique. *Phytochemistry* **2004**, *65*, 857–864.

(25) Xie, G. X.; Ni, Y.; Su, M. M.; Zhang, Y. Y.; Zhao, A. H.; Gao, X. F.; Liu, Z.; Xiao, P. G.; Jia, W. Application of ultra-performance LC-TOF MS metabolite profiling techniques to the analysis of medicinal *Panax* herbs. *Metabolomics* **2008**, *4*, 248–260.

(26) Pongsuwan, W.; Bamba, T.; Harada, K.; Yonetani, T.; Kobayashi, A.; Fukusaki, E. High-throughput technique for comprehensive analysis of Japanese green tea quality assessment using ultra-performance liquid chromatography with time-of-flight mass spectrometry (UPLC/TOF MS). *J. Agric. Food Chem.* **2008**, *56*, 10705–10708.

(27) Dettmer, K.; Aronov, P. A.; Hammock, B. D. Mass spectrometry-based metabolomics. *Mass Spectrom. Rev.* **2007**, *26*, 51–78.

(28) Ralston-Hooper, K.; Hopf, A.; Oh, C.; Zhang, X.; Adamec, J.; Sepulveda, M. S. Development of GC×GC/TOF-MS metabolomics for use in ecotoxicological studies with invertebrates. *Aquat. Toxicol.* **2008**, *88*, 48–52.

(29) Little, D.; Plumb, R. *Waters Corporation, Application Note 720001120EN-KJ*, 2005.

(30) *Agilent Technologies, Application Note 5989-2108EN*, 2005.

(31) Nordstrom, A.; O'Maille, G.; Qin, C.; Siuzdak, G. Nonlinear data alignment for UPLC-MS and HPLC-MS based metabolomics: quantitative analysis of endogenous and exogenous metabolites in human serum. *Anal. Chem.* **2006**, *78*, 3289–3295.

(32) Wilson, I. D.; Nicholson, J. K.; Castro-Perez, J.; Granger, J. H.; Johnson, K. A.; Smith, B. W.; Plumb, R. S. High resolution "ultra performance" liquid chromatography coupled to oa-TOF mass spectrometry as a tool for differential metabolic pathway profiling in functional genomic studies. *J. Proteome Res.* **2005**, *4*, 591–598.

(33) Shen, Y.; Zhang, R.; Moore, R. J.; Kim, J.; Metz, T. O.; Hixson, K. K.; Zhao, R.; Livesay, E. A.; Udseth, H. R.; Smith, R. D. Automated 20 kpsi RPLC-MS and MS/MS with chromatographic peak capacities of 1000−1500 and capabilities in proteomics and metabolomics. *Anal. Chem.* **2005**, *77*, 3090–3100.

(34) http://www.kemco.or.kr/web/kem_class/middleschool/middleschool0404.asp.

(35) Kullgren, A.; Samuelsson, L. M.; Larsson, D. G.; Bjornsson, B. T.; Bergman, E. J. A metabolomics approach to elucidate effects of food deprivation in juvenile rainbow trout (*Oncorhynchus mykiss*). *Am. J. Physiol.: Regul., Integr. Comp. Physiol.* **2010**, *299*, R1440–R1448.

(36) Trygg, J.; Holmes, E.; Lundstedt, T. Chemometrics in metabonomics. *J. Proteome Res.* **2007**, *6*, 469–479.

(37) Wiklund, S.; Johansson, E.; Sjostrom, L.; Mellerowicz, E. J.; Edlund, U.; Shockcor, J. P.; Gottfries, J.; Moritz, T.; Trygg, J. Visualization of GC/TOF-MS-based metabolomics data for identification of biochemically interesting compounds using OPLS class models. *Anal. Chem.* **2008**, *80*, 115–122.

(38) Hong, Y. S.; Ahn, Y. T.; Park, J. C.; Lee, J. H.; Lee, H.; Huh, C. S.; Kim, D. H.; Ryu, D. H.; Hwang, G. S. ^{1}H NMR-based metabonomic assessment of probiotic effects in a colitis mouse model. *Arch. Pharm. Res.* **2010**, *33*, 1091–1101.

(39) Kang, J.; Choi, M. Y.; Kang, S.; Kwon, H. N.; Wen, H.; Lee, C. H.; Park, M.; Wiklund, S.; Kim, H. J.; Kwon, S. W.; Park, S. Application of a ^{1}H nuclear magnetic resonance (NMR) metabolomics approach combined with orthogonal projections to latent structure—discriminant analysis as an efficient tool for discriminating between Korean and Chinese herbal medicines. *J. Agric. Food Chem.* **2008**, *56*, 11589–11595.

(40) Wen, H.; Yoo, S. S.; Kang, J.; Kim, H. G.; Park, J. S.; Jeong, S.; Lee, J. I.; Kwon, H. N.; Kang, S.; Lee, D. H.; Park, S. A new NMR-based metabolomics approach for the diagnosis of biliary tract cancer. *J. Hepatol.* **2010**, *52*, 228–233.

(41) Ahn, M.-J.; Lee, M. K.; Kim, Y. C.; Sung, S. H. The simultaneous determination of coumarins in *Angelica gigas* root by high performance liquid chromatography-diode array detector coupled with electrospray ionization/mass spectrometry. *J. Pharm. Biomed. Anal.* **2008**, *46*, 258–266.

(42) Lee, S. H.; Lee, Y. S.; Jung, S. H; Shin, K. H; Kim, B. K.; Kang, S. S. Anti-tumor activities of decursinol angelate and decursin from *Angelica gigas*. *Arch. Pharm. Res.* **2003**, *9*, 727–730.

(43) Yoo, H. H.; Lee, M. W.; Kim, Y. C.; Yun, C. H.; Kim, D. H. Mechanism-based inactivation of cytochrome P450 2A6 by decursinol angelate isolated from *Angelica gigas*. *Drug Metab. Dispos.* **2007**, *35*, 1759–1765.

(44) Bahrami, A. R.; Chen, Z.-H.; Walker, R. P.; Leegood, R. C.; Gray, J. E. Ripening-related occurrence of phosphoenolpyruvate carboxykinase in tomato fruit. *Plant Mol. Biol.* **2001**, *47*, 499–506.

(45) Ruffner, H. P.; Brem, S.; Rast, D. M. Pathway of photosynthetic malate formation in *Vitis vinifera*, a C3 plant. *Plant Physiol.* **1983**, *73*, 582–585.

(46) Ruffner, H. P.; Kliewer, W. M. Phosphoenolpyruvate carboxykinase activity in grape berries. *Plant Physiol.* **1975**, *56*, 67–71.

(47) Ruffner, H. P.; Hawker, J. S.; Hale, C. R. Temperature and enzymic control of malate metabolism in berries of *Vitis vinifera*. *Phytochemistry* **1976**, *15*, 1877–1880.

(48) Luna kova, L.; Masarovi ova, E.; Lux, A. Respiration rate and chemical composition of *Karwinskia* roots as affected by temperature. *Biol. Plant.* **2000**, *43*, 611–613.

(49) Lux, D.; Leonardi, S.; Müller, J.; Wiemken, A.; Flückiger, W. Effects of ambient ozone concentrations on contents of non-structural carbohydrates in young *Picea abies* and *Fagus sylvatica*. *New Phytol.* **1997**, *137*, 399–409.

(50) Covey-Crump, E. M.; Attwood, R. G.; Atkin, O. K. Regulation of root respiration in two species of Plantago that differ in relative growth rate: the effect of short- and long-term changes in temperature. *Plant, Cell Environ.* **2002**, *25*, 1501–1513.